Electronic Supplementary Material (ESI) for Journal of Materials Chemistry A.

Supplementary Information

Iterative oxidation and sulfidation reactions: Revival of bulk cobalt sulfide into an active electrocatalyst for the oxygen evolution reaction

Min Soo Kim[a†], Malenahalli Halappa Naveen[b†], Rizwan Khan[a] and Jin Ho Bang*[abc]

[a]*Department of Bionano Technology, Hanyang University, 55 Hanyangdaehak-ro, Sangnok-gu, Ansan, Gyeonggi-do 15588, Republic of Korea*

[b]*Nanosensor Research Institute, Hanyang University, 55 Hanyangdaehak-ro, Sangnok-gu, Ansan, Gyeonggi-do 15588, Republic of Korea*

[c]*Department of Chemical and Molecular Engineering and Department of Applied Chemistry, Hanyang University, 55 Hanyangdaehak-ro, Sangnok-gu, Ansan, Gyeonggi-do 15588, Republic of Korea*

Author Contributions:

[†]These authors contributed equally to this work.

*Corresponding Author

E-mail: jbang@hanyang.ac.kr

Experimental

Synthesis of bulk CoS_x and the thermal process for re-engineering

$Co(OH)_2$ microspheres serving as a precursor of bulk CoS_x were produced by a co-precipitation method, where an aqueous solution of $CoSO_4 \cdot 7H_2O$ was added dropwise to a solution containing NH_4OH and NaOH at a pH of 10.95 under vigorous stirring for 48 h. The prepared $Co(OH)_2$ was subjected to heat treatment at 550 °C for 3 h under H_2S gas (10% in Ar) flow to obtain the bulk CoS_x microspheres. The resulting CoS_x was re-engineered through repeated oxidation and sulfidation processes. For the oxidation, it was sintered at 800 °C for 5 h under air to produce Co_3O_4. The obtained Co_3O_4 was further subjected to heat treatment at 450 °C under H_2S gas for 1 h, which restored the crystal structure to CoS_x. This oxidation/sulfidation process was repeated four times under the same reaction conditions, as illustrated in Scheme S1.

Characterization

The morphology of materials yielded after each thermal process was examined by scanning electron microscopy (SEM, Tescan VEGA3) and cross-sectional SEM images of a focused ion beam (FIB)-milled CoS_x particle were obtained using a combined SEM/FIB microscope (Quanta 3D FEG, FEI). X-ray diffraction (XRD) patterns were acquired by an X-ray diffractometer (Rigaku D/Max-2500/PC). A surface area analyzer (BELSORP-mini II, BEL Japan) was used to measure N_2 physisorption isotherms at 77.4 K. The specific surface area was determined by the Brunauer–Emmett–Teller (BET) method and the pore size distributions were obtained using the Barrett–Joyner–Halenda (BJH) method. AutoPore V 9600 (Micromeritics) was used for the mercury porosimetry analysis. Thermogravimetric analysis (TGA) and differential scanning calorimetry (DSC) were performed using a thermal analyzer (SDT-Q600, TA Instrument) ramped at 10 $°C \cdot min^{-1}$ under an airflow of 100 $mL \cdot min^{-1}$. The surface analysis of sf4-CoS_x was performed by X-ray photoelectron spectroscopy (XPS, PHI Versa Probe system).

Electrochemical measurements

All electrochemical experiments were performed using a CHI potentiostat (660D) connected with a three-electrode system. A CoS_x-modified glassy carbon (GC) electrode was used as the working electrode while a Hg/HgO electrode and Pt wire used as the reference and the counter electrodes, respectively. OER measurements were carried out using 1 M KOH as the electrolyte. To prepare catalyst inks, 5 mg of each active catalyst was dispersed in 1 mL of an ethanol:deionized water mixture (1:1) containing 10 µL of 5 wt% Nafion (Aldrich) and then sonicated for 1 h. To fabricate the working electrode, an aliquot of the catalyst ink (catalyst loading of 50 µg) was drop-casted onto a polished GC electrode and dried at room temperature. As a control, IrO_2 powder (99%, Alfa Aesar) was used (see the characterization results of IrO_2 in Figure S1) and a catalyst ink was prepared using the same procedure as the CoS_x catalysts. As the potential is pH-dependent, all measured potentials against the Hg/HgO reference electrode were converted into the reversible hydrogen electrode (RHE) and they were also *iR*-compensated. Electrochemical double-layer capacitance (C_{dl}) was calculated using cyclic voltammetry (CV) measured at different scan rates to determine the electrochemical surface area (ECSA) of each catalyst. The potential range where no Faradaic process occurred was selected. The C_{dl} was calculated as the slope of the linear relationship between the current density and scan rate. To calculate ECSA (ECSA = $R_f \times S$, S is the geometric area of the electrode), the roughness factor (R_f) of each catalyst was determined from the ratio of C_{dl} and the geometrical surface area of a bare GC electrode. The turnover frequency (TOF) was estimated according to the following equation: TOF = $(j \times A)/4nF$, where j is the geometrical current density at an overpotential of 400 mV, A is the surface area of the GC electrode (0.196 cm^2), n is the number of moles of metal atoms in a catalyst, and F is the Faraday constant. For the TOF calculation, it was assumed that all of the metal atoms in CoS_x and IrO_2 were catalytically active for the OER. Electrochemical impedance spectroscopy (EIS) measurements were carried out in the frequency range of 1 kHz to 10 mHz with a 5 mV perturbation.

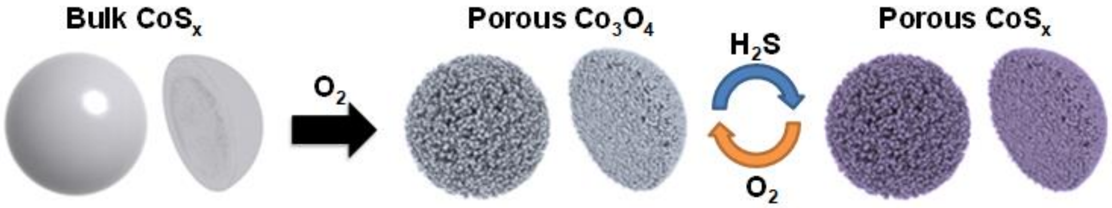

Scheme S1 Re-engineering process of bulk CoS_x through iterative oxidation/sulfidation reactions.

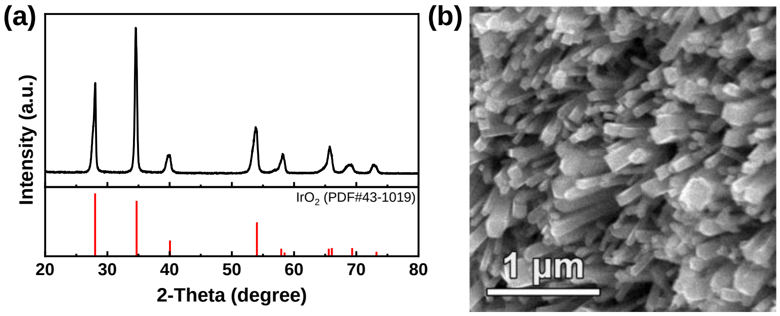

Fig. S1 (a) XRD pattern and (b) SEM image of commercial IrO_2.

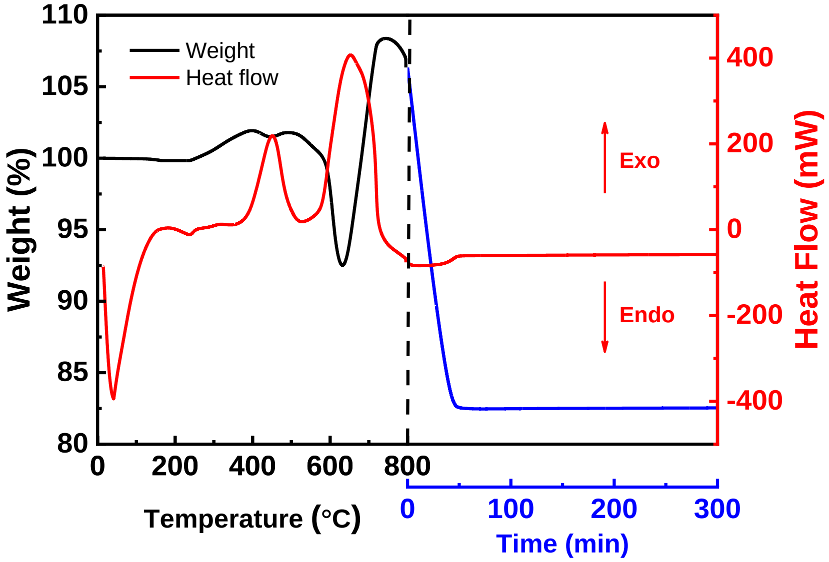

Fig. S2 TGA/DSC analysis of CoS_x under oxidation in air. The decomposition mechanism of CoS_x remains elusive and, given the complex phase transformations involved in this process as revealed by our *ex situ* XRD analysis, it is very difficult to ascertain the mechanism. However, based on the *ex situ* XRD analysis and several reports in the literature,[1,2] we speculated that the following reaction process may be plausible. The initial small weight loss up to 200 °C is attributed to SO_2 formation.[1] The weight gains at temperatures of ~380 and ~480 °C are known to be associated with O_2 uptake, which is followed by a weight loss at ~600 °C. The weight gain up to ~700 °C is presumably associated with the formation of $CoSO_4$ and the dramatic weigh loss when the temperature was held at 800 °C for 5 h is ascribed mainly to the decomposition of $CoSO_4$ into Co_3O_4.[2]

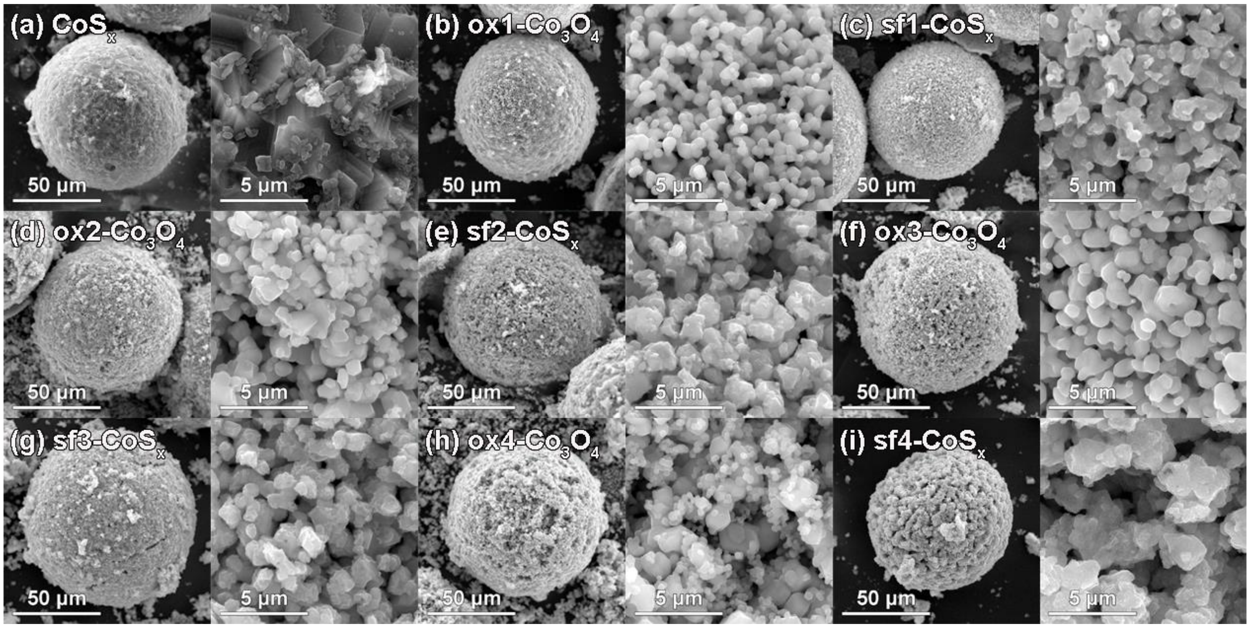

Fig. S3 SEM images (taken at both low and high magnifications) of CoS$_x$ obtained at various reaction stages: (a) CoS$_x$, (b) ox1-Co$_3$O$_4$, (c) sf1-CoS$_x$, (d) ox2-Co$_3$O$_4$, (e) sf2-CoS$_x$, (f) ox3-Co$_3$O$_4$, (g) sf3-CoS$_x$, (h) ox4-Co$_3$O$_4$, and (i) sf4-CoS$_x$.

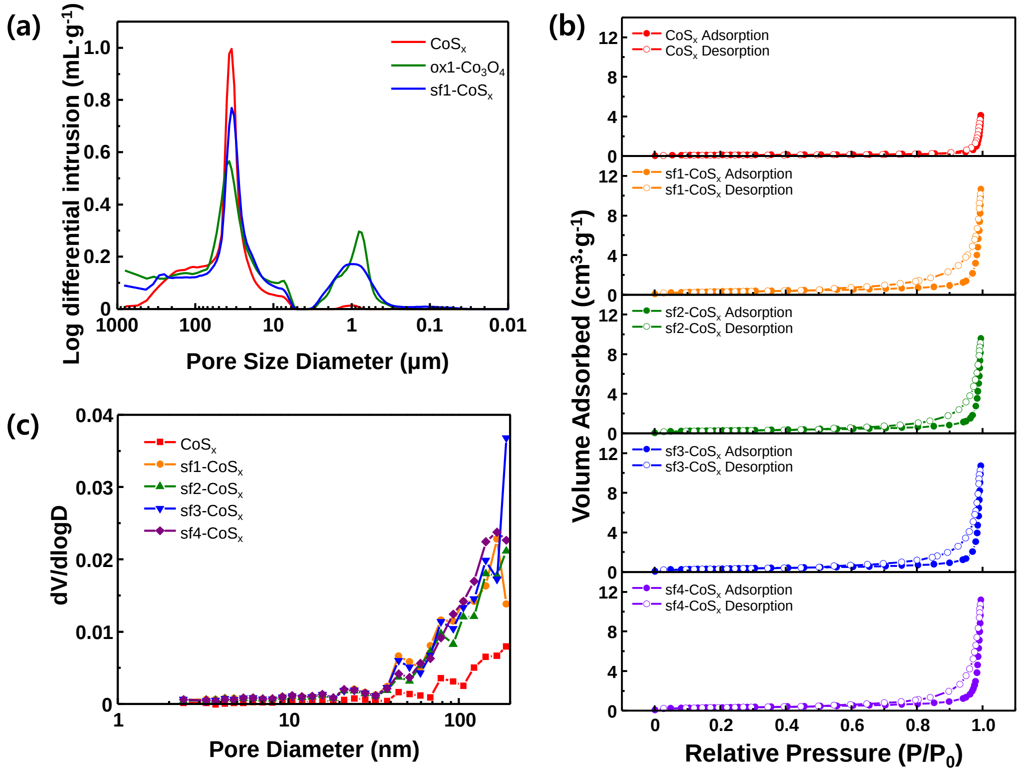

Fig. S4 (a) Mercury porosimetry results of bulk CoS$_x$, ox1-CoS$_x$, and sf1-CoS$_x$. (b) N$_2$ physisorption isotherms and (c) pore size distribution of bulk CoS$_x$, sf1-CoS$_x$, sf2-CoS$_x$, sf3-CoS$_x$, and sf4-CoS$_x$.

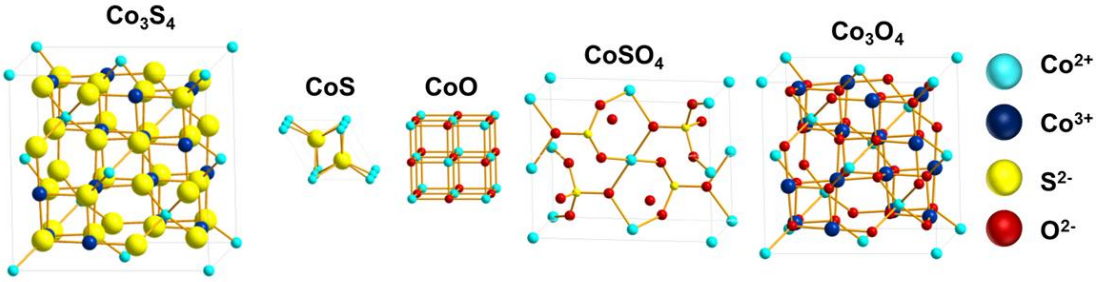

Fig. S5 Unit cell structures of cobalt sulfides, oxides, and sulfate.

Table S1 Crystal structures and lattice parameters of cobalt sulfides, oxides, and sulfate.

	Crystal Structure	**Lattice Parameters (Å)**			**Unit Cell Volume ($Å^3$)**	**Density ($g \cdot cm^{-3}$)**
		a	***b***	***c***		
Co_3S_4	Cubic	9.41	9.41	9.41	832.0	4.65
CoS	Hexagonal	3.38	3.38	5.15	50.9	5.94
CoO	Cubic	4.26	4.26	4.26	77.3	6.44
$CoSO_4$	Orthorhombic	8.61	6.71	4.74	273.8	3.76
Co_3O_4	Cubic	8.08	8.08	8.08	528.2	6.06

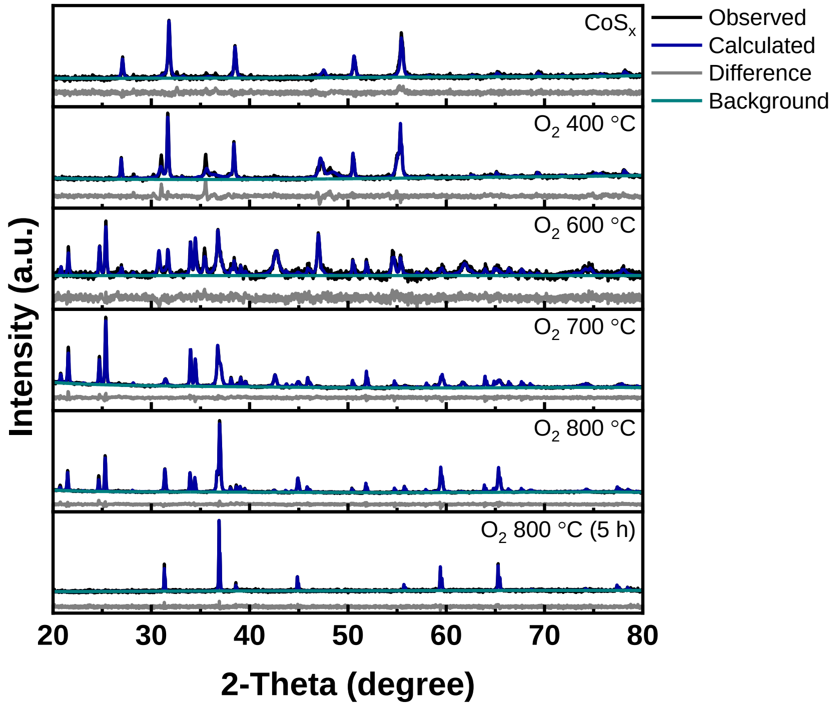

Fig. S6 Rietveld refinement of the XRD patterns of bulk CoS_x and reaction intermediates obtained during oxidation.

$$Co_3S_4 + O_2 \rightarrow 3CoS + SO_2\uparrow$$
$$2CoS + 3O_2 \rightarrow 2CoO + 2SO_2\uparrow$$
$$6CoO + O_2 \rightarrow 2Co_3O_4$$

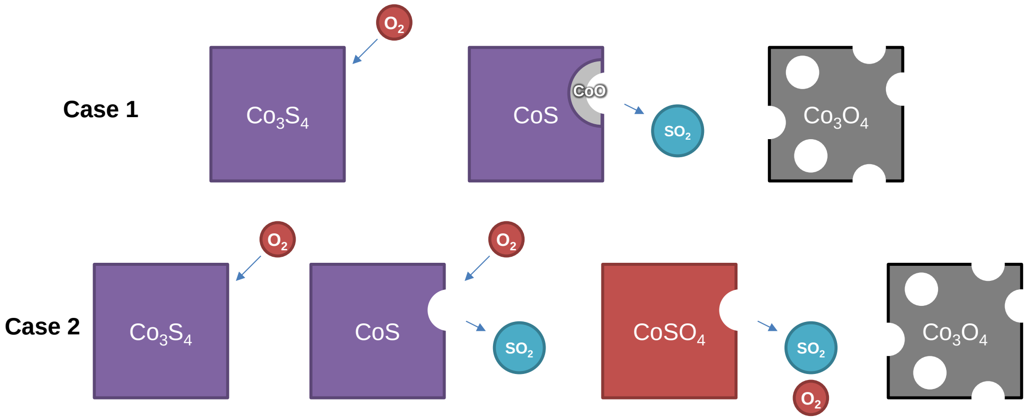

$$Co_3S_4 + O_2 \rightarrow 3CoS + SO_2\uparrow$$
$$CoS + 2O_2 \rightarrow CoSO_4$$
$$3CoSO_4 \rightarrow Co_3O_4 + 3SO_2\uparrow + O_2\uparrow$$

Scheme S2 Schematic illustration of possible mechanisms for the formation of Co_3O_4 by oxidation of bulk CoS_x.

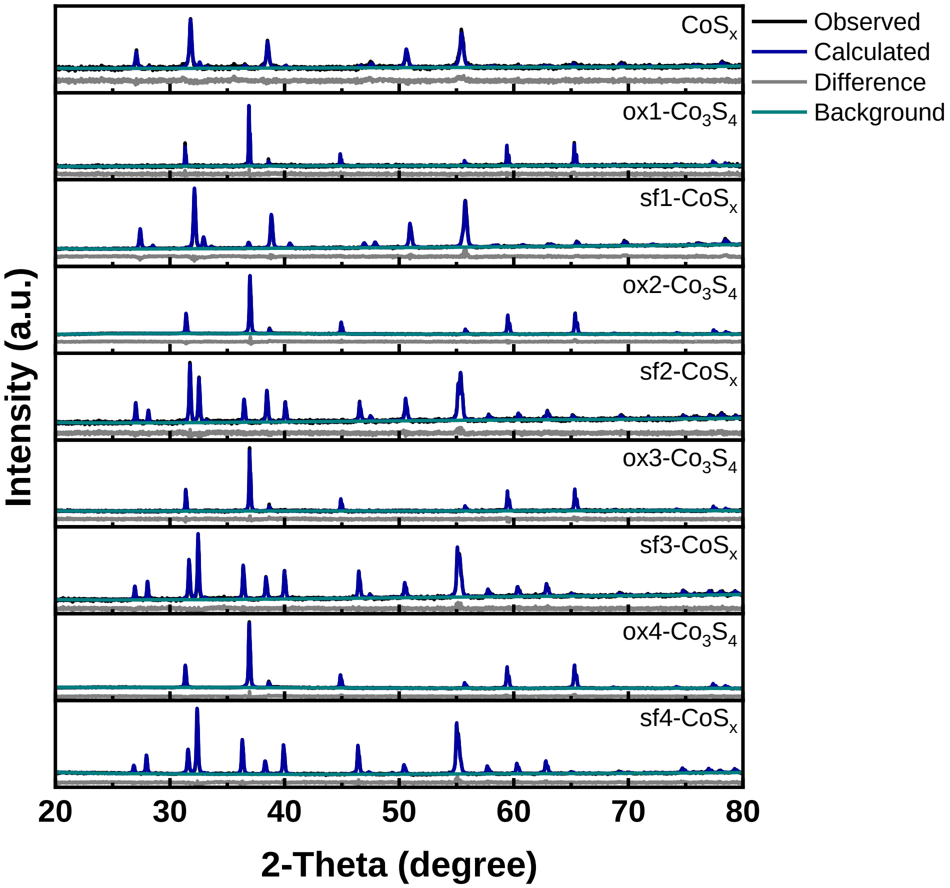

Fig. S7 Rietveld refinement of the XRD patterns of various products yielded during repetitive oxidation/sulfidation reactions.

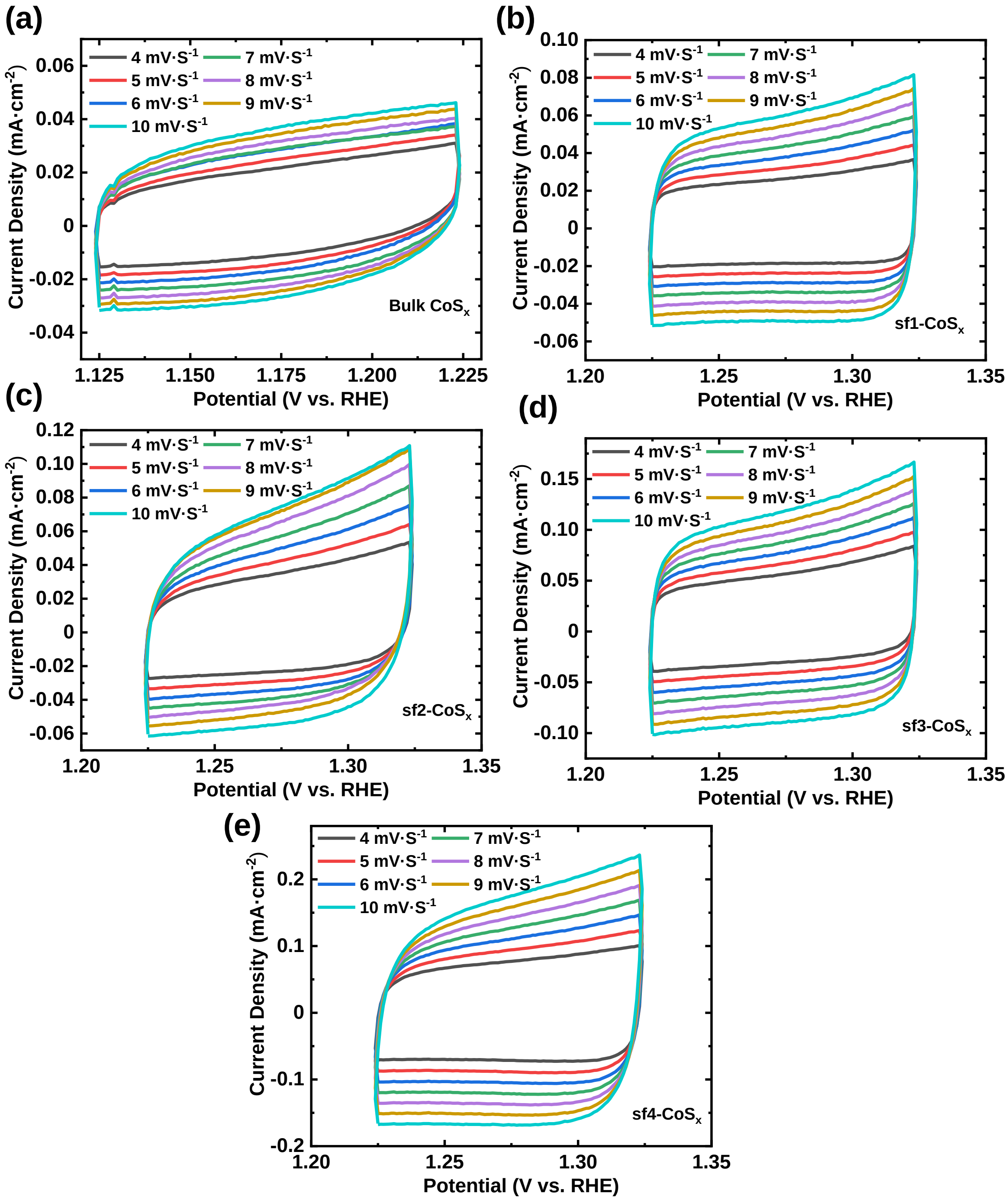

Fig. S8 Cyclic volatamograms of (a) bulk CoS_x, (b) sf1-CoS_x, (c) sf2-CoS_x, (d) sf3-CoS_x, and (e) sf4-CoS_x at different scan rates.

Table S2 Electrochemical double-layer capacitance (C_{dl}), roughness factor (R_f), and electrochemical surface area (ECSA) of each catalyst. Charge transfer resistance (R_{ct}) determined by EIS analysis and turnover frequency (TOF).

Electrode Material	C_{dl} (mF•cm^{-2})	R_f	ECSA (cm^2)	R_{ct} (Ω)	TOF (ms^{-1})
Bulk CoS_x	2.40	14.83	2.90	747.8	4.08
sf1-CoS_x	5.53	34.18	6.70	590.6	6.37
sf2-CoS_x	6.73	41.60	8.15	365.3	7.96
sf3-CoS_x	10.13	62.61	12.27	211.3	15.09
sf4-CoS_x	15.82	97.79	19.16	192.0	21.36

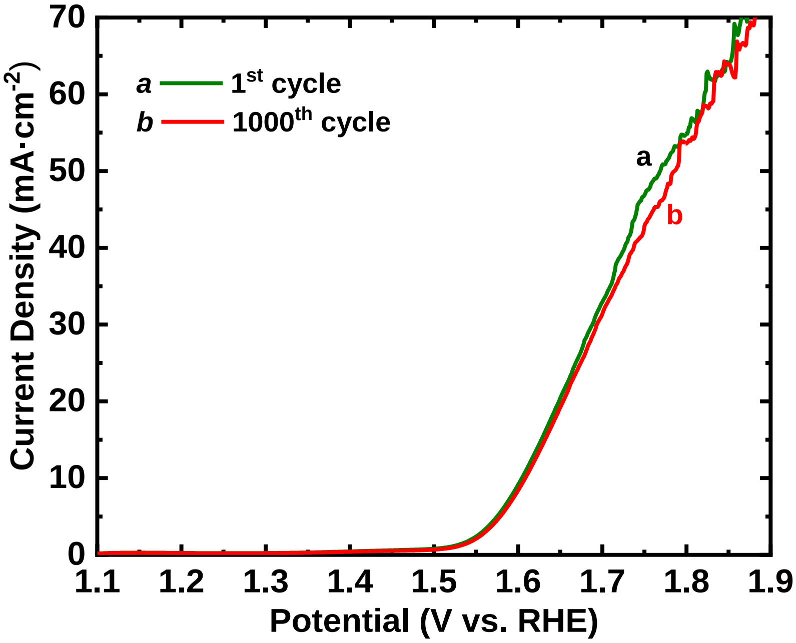

Fig. S9 LSV curves of sf4-CoS_x (a) before and (b) after 1,000 CV scans at a scan rate of 50 mV·s^{-1}.

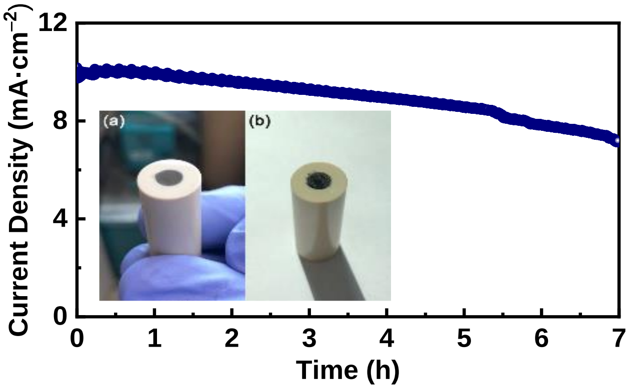

Fig. S10 Chronoamperogram of sf4-CoS$_x$ measured at an overpotential of 0.375 V. There is a gradual current decline over time, which primarily resulted from the detachment of sf4-CoS$_x$ off of the GC electrode due to limited binding strength offered by Nafion as shown in the inset (photos of the working electrode (a) before and (b) after the long-term test).

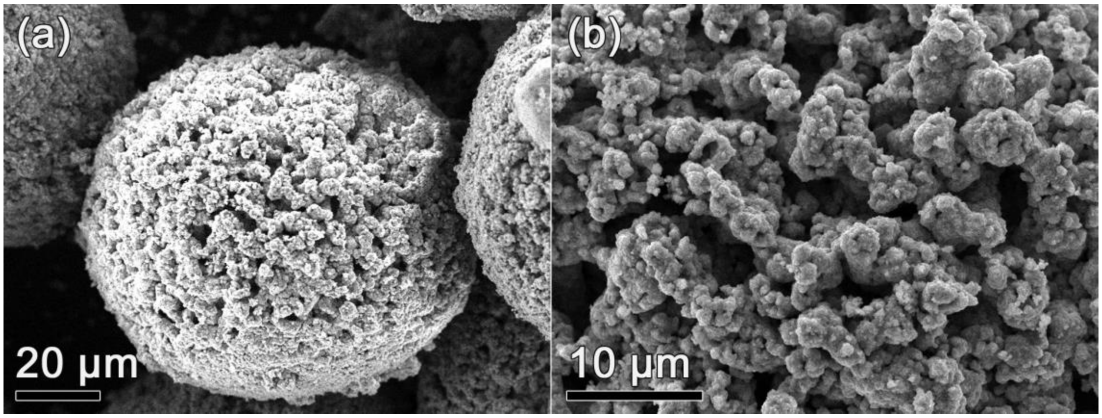

Fig. S11 SEM images of sf4-CoS$_x$ (a) before and (b) after the OER test performed by chronoamperometry.

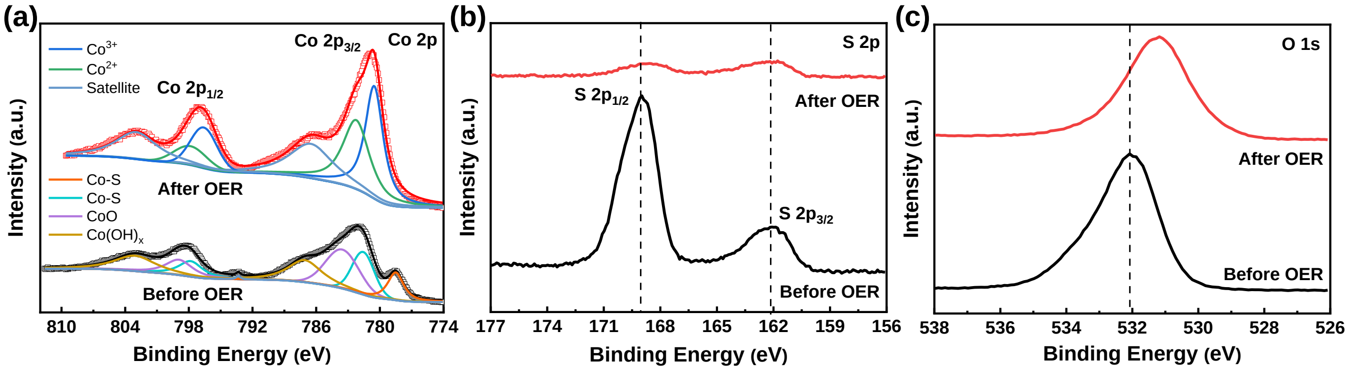

Fig. S12 XPS spectra of sf4-CoS$_x$ before and after OER test: (a) Co 2p, (b) S 2p, and (c) O 1s.

References

1 Y. Yoshimura, N. Matsubayashi, H. Yokokawa, T. Sato, H. Shimada and A. Nishijima, *Ind. Eng. Chem. Res.*, 1991, **30**, 1092-1099.

2 T. R. Ingraham and P. Marier, *Thermochim. Acta*, 1970, **1**, 39-49.